ISSN 1068-3739, Russian Meteorology and Hydrology, 2015, Vol. 40, No. 6, pp. 392–399. Allerton Press, Inc., 2015.
Original Russian Text D.V. Kulyamin, V.Ya. Galin, A.I. Pogoreltsev, 2015, published in Meteorologiya i Gidrologiya, 2015, No. 6, pp. 48–57.

The Thermosphere General Circulation Modeling with the Parametrization of Radiative Processes

D. V. Kulyamin[a, b, c], V. Ya. Galin[b], A. I. Pogoreltsev[d]

[a]*Research Computing Center of Lomonosov Moscow State University, Leninskie Gory 1, stroenie 4, Moscow, 199034 Russia, e-mail: kulyamind@mail.ru*

[b]*Institute of Applied Physics, Russian Academy of Sciences, ul. Rostokinskaya 9, Moscow, 129128 Russia*

[c]*Institute of Numerical Mathematics, Russian Academy of Sciences, ul. Gubkina 8, Moscow, 119333 Russia*

[d]*Russian State Hydrometeorological University, Malookhtinsky pr. 98, St. Petersburg, 195196 Russia*

Received February 9, 2015

Abstract—The paper presents a new version of the global three-dimensional general circulation model of the Earth's thermosphere (90–500 km) with high spatial resolution (2 2.5 80), including consistent calculation of radiative processes. Based on a detailed analysis of the reproduction of the various components of radiation transfer a good agreement of radiation balance with empirical data is shown in the new model. Analytical estimations and model results proved that the thermosphere global state formation is essentially determined by the ratio between the radiation heating and heat sink due to molecular parameters, as well as by the lower boundary conditions. On the base of the preliminary model identification with empirical data a satisfactory reproduction of the thermal balance and the thermospheric general circulation features is shown.

DOI: 10.3103/S1068373915060059

Keywords: Mathematical modeling, thermosphere, atmospheric radiation, ultraviolet solar radiation, atmospheric general circulation

1. INTRODUCTION

Present-day interest in the upper atmosphere modeling is caused by a large number of challenges in various fields, such as radio physics, space research, solar terrestrial relations and the role of the upper atmosphere in the Earth's climate formation. One approach to this problem is to improve current climate models by describing the upper atmospheric layers. Currently this approach is implemented as a part of the development of the high-level resolution model of the Earth system; this work is carried out at the Institute of Numerical Mathematics of Russian Academy of Sciences (INM RAS) [10]. The first in Russia who turned to the numerical modeling of near-Earth processes was G.I. Marchuk, the founder of INM RAS [1].

The first version of the three-dimensional model of general thermospheric circulation (for the altitudes from 90 to 500 km) with a high spatial resolution (as a computational block of the Earth system model under development) was created by the authors [9]. This model used simple approximations for the calculation of key physical processes. In the work first stage the main emphasis was put on the numerical implementation of the model dynamic core and on the satisfactory reproduction of the main peculiarities of global thermospheric circulation. It was highlighted that in the further model development the key step was the correct description of radiative processes. They determine the structure of thermospheric global circulation (a sharp growth of temperature with altitude, atmospheric tides prevailing in the dynamics etc.) as well as energy of photochemical transformations (causing the ionosphere formation, the inhomogeneity of gas composition and other phenomena). Constructing accurate parameterization for the calculation of the rates of thermospheric heating and cooling due to radiation transport is a separate problem.

The main difficulty lies in the correct description of the complex mechanisms of energy conversion in the upper atmosphere. Studies on the thermospheric radiation balance and corresponding numerical estimations of heat sources and sinks from different physical mechanisms have been carried out since the 1970s using the analysis of aeronomical and satellite measurements as well as the construction of simple empirical models and general circulation models [8, 16, 18]. The key energy source for the thermosphere is the absorption of the short-wave solar radiation [11]. This process is responsible for the ionization or dissociation of major gas components (atomic oxygen, molecular nitrogen and oxygen) thus initiating photochemical transformations and creating the Earth's ionosphere (which interacts with neutral particles).

Neutral gas heating in the upper thermosphere (above 170 km) is determined by the transfer of the energy of hard ionizing solar radiation primarily through the elastic and inelastic collisions of photoelectrons and ions with neutrals as well as through nonadiabatic chemical interactions, secondary radiation and metastable quenching of exited states etc. [2, 16]. Traditionally an effective portion of the absorbed solar short-wave radiation energy transformed into heat, is estimated for the numerical calculation of the net neutral gas heating rate [11, 16].

Heating of neutral gas in the lower thermosphere (from 90 to 170 km) is determined mainly by photodissociative absorption of far ultraviolet solar radiation by molecular oxygen, as well as by nitrogen and mesospheric ozone absorption and energy transfer through chemical reactions (atomic oxygen recombination etc.) [19, 21]. We should point out a significant difference in optical properties between the upper and lower layers of the thermosphere: the upper layers are in fact optically transparent, and heating there is nonlocal and uniform with a high contrast between the day (when illuminated by the sun) and night; the lower thermosphere is optically thick, and heating is more local and determined by complex radiation balance. Long-wave thermal radiation by thermospheric components is relatively small, however it is a key process on the heights of the middle atmosphere (from 90 to 150 km) and significantly contributes to the total radiation balance due to molecular thermal conductivity and turbulent mixing [8, 16]. At these altitudes the cooling is determined by infrared nonlocal thermodynamic equilibrium (non-LTE) radiation (primarily by carbon dioxide emission and closer to the mesosphere, by the emissions of nitric oxide and other components) [5].

Thus, we can formulate several primary problems whose solution requires the global thermosphere model development with the consistent calculation of radiative processes:

—correct reproduction of the radiation balance in the model and investigation of the relative role of radiation, dissipation and dynamical processes in the thermospheric global state formation (here we consider the formation of the mean temperature profile and its temporal and structural variability);

—reproduction of the structure of thermosphere general circulation and examination of the role of radiative processes in the formation of its spatial and temporal characteristics.

This paper is dedicated to the improvement of the thermospheric general circulation model [9] by inclusion of the consistent calculation of radiative heating and cooling. The main focus is given to the proper representation of the global radiation balance in the upper atmosphere and the resulting general circulation.

2. THE THERMOSPHERIC GENERAL CIRCULATION MODEL

The considered model of the thermosphere solves a system of nonlinear primitive equations of the atmosphere hydrothermodynamics written in a spherical system of coordinates with a normalized isobaric vertical coordinate [9]. Since the new version of the model includes the calculation of the total radiation balance, its main difference from the previous one lies rather in reformulated equations where the temperature T and geopotential variables are calculated in the full form, than in deviations from a mean profile.

The system of equations has the following form:

$$\frac{du}{dt} \quad f \quad \frac{u}{a}\mathrm{tg} \quad v \quad \frac{1}{a\cos} \quad \frac{}{} \quad g^2 \frac{}{p} \quad \frac{u}{p} \quad \frac{RT}{p}(D_{xx}u \quad D_{xy}v),$$

$$\frac{dv}{dt} \quad f \quad \frac{u}{a}\mathrm{tg} \quad u \quad \frac{1}{a} \quad \frac{}{} \quad g^2 \frac{}{p} \quad \frac{u}{p} \quad \frac{RT}{p}(D_{yy}v \quad D_{xy}u),$$

$$\frac{}{p} \quad \frac{RT}{p}, \tag{1}$$

$$\frac{dT}{dt} \quad \dot{p}\frac{RT}{pc_p} \quad \frac{g^2}{c_p} \frac{}{p} \quad \frac{T}{p} \quad ,$$

$$\frac{1}{a\cos}\;\frac{u}{}\;\frac{v\cos}{}\qquad\frac{\dot{p}}{p}\quad 0$$

where $\dfrac{d}{dt}\quad\dfrac{}{t}\quad\dfrac{u}{a\cos}\dfrac{}{}\quad\dfrac{v}{a}\dfrac{}{}\quad\dot{p}\dfrac{}{p};\ \dot{p}\quad dp/dt;\qquad\dfrac{p}{RT}$ is gas density.

In system (1) the independent variables are longitude, latitude, time and pressure (, , t, p), u, v are horizontal velocity components, 10^{-3} p 4 10^{-10} hPa [9]. The right-hand sides of the equations of motion and heat flow include the rates or momentum and internal energy variation caused by subgrid-scale physical processes that determine the global state of the thermosphere and are calculated by the corresponding parameterizations. is the total heating rate due to radiation processes and is calculated using a developed radiation block.

The dynamical interaction of the thermosphere and the ionosphere is taken into account by the ion-neutral drag force parameterization for horizontal wind velocity components in the so called diffusive approximation (the second term on the right side of motion equations). The two-dimensional ion-drag tensor D is determined according to the previous model version [9]. Since a developed version of the thermospheric model has a new radiation block, a separate calculation of Joule heating due to ion-neutral collisions is not performed.

The first term on the right-hand sides of temperature and motion equations (1) describes the processes of vertical diffusion and thermal conductivity. The coefficients and $_{\mathrm{mol}}$ that define molecular diffusive processes for the upper thermosphere are set according to [9]. Since the model new version consistently solves the equation for full temperature, it is necessary to consider the impact of the turbulent mixing associated with internal gravity waves (extending from the mesosphere) for the correct reproduction of the lower thermosphere thermal balance [2, 8, 16]. Creation of appropriate parameterization is a separate complex problem and lies beyond the scope of this paper [7]. As this version of thermospheric model ignores the direct dynamical interaction with the mesosphere, in the first approximation this process is considered only for temperature by introduction of an additional term to the thermal conductivity, so that the total coefficient is defined as $_{\mathrm{mol}}\quad K_D(p)$ ($K_D = 10^3$ m^2/s at the lower boundary and decreases linearly with altitude which corresponds to the empirical and model estimates [2, 7]).

The lower boundary condition for full temperature in the heat flow equation is given by the constant value of mean mesospheric temperature $T_0 = 180$ K for simplicity. The corresponding upper boundary condition is of a particular interest because such kind of equations with the isobaric coordinate system traditionally uses a degenerate upper level $p = 0$.

It is well known that the observed vertical profile of temperature in the upper thermosphere corresponds closely to the stationary solution of the equation of heating and thermal conductivity balance which can be written as:

$$\frac{g^2}{c_p}\,\frac{}{p}\,\frac{p}{R\overline{T}}\,\frac{\overline{T}}{p}\qquad {}_0. \tag{2}$$

Assuming $_0$ = const and setting boundary conditions for some lower level is $p = p_b$ (typically around 120 km): $\overline{T} = T_b$ and for the upper level $p = 0$: $\overline{T}\quad T$, the solution of (2) is expressed by a linear dependence $\overline{T}_{(p)}\quad T\quad p(T\quad T_b)/p_b$ [6]. In this case the singularity at the upper boundary determines the nonlinear relationship between exosphere temperature T and radiation heating in the upper thermosphere:

$$_0\quad\frac{(T\quad T_b)}{p_b}\,\frac{g^2}{RT}. \tag{3}$$

Therefore, when modeling the thermospheric global state it is not correct to use the Dirichlet boundary condition $T = T$ for the degenerate upper level. In this work we use the radiative boundary condition so that the temperature at the upper layers is determined from the relation of the model parameters of form (3).

The main features of model numerical implementation and values of the used parameters are detailed in [9]. The model contains 80 vertical levels and its spatial horizontal resolution is 2 2.5 . The model code has been developed for parallel computing, the reported study was supported by the Supercomputing Center of Lomonosov Moscow State University.

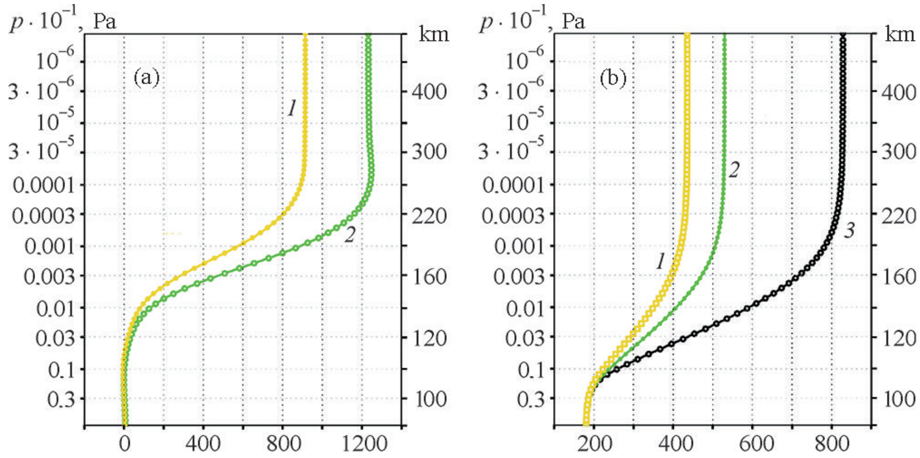

Fig. 1. (a) The global mean vertical profiles of the neutral heating rate ‾ (K/day) and (b) temperature $\bar{T}$ (K) according to the modeling of thermospheric general circulation for different model parameters: (*1*) $\mathrm{eff}_{\mathrm{EUV}} = 0.36$; (*2*) $\mathrm{eff}_{\mathrm{EUV}} = 0.5$; (3) $\mathrm{eff}_{\mathrm{EUV}} =$ $= 0.36$, $= 0.5\ _0$.

3. CALCULATION OF RADIATIVE HEAT TRANSFER

To solve the main problem of the consistent calculation of heating and cooling in the thermosphere we have used the radiation numerical block developed for the Middle and Upper Atmosphere Model (MUAM) [12].

The calculation of neutral gas heating is based on the classic parameterization [21] with slight modifications performed according to [19]. In this version of the radiation block for thermospheric altitudes the following heating radiative processes are taken into account: heating due to the absorption of extreme ultraviolet (EUV) solar radiation (5–105 nm) by atomic oxygen O, molecular oxygen O_2 and nitrogen N_2; heating due to photodissociative absorption of ultraviolet (UV) radiation in Schumann–Runge bands (175–205 nm), in the Schumann–Runge continuum (125–175 nm), in the Lyman-alpha line (121 nm), as well as in the Herzberg continuum (205–245 nm); absorption by mesospheric ozone O_3 in Hartley bands (200–300 nm) and the Herzberg continuum (205–245 nm) is also accounted. For molecular and atomic oxygen the heating associated with certain chemical transformations is taken into account separately [19]. The solar EUV flux F_{EUV} and the corresponding cross sections of absorption are calculated in 37 spectral intervals using EUVAC parameterization [14]. Solar activity is taken on an average level. For the results considered here we used several different values of the heating efficiency of solar EUV radiation ($\mathrm{eff}_{\mathrm{EUV}} = 0.36$ which corresponds to the value used in [4, 16] and simplifies the comparison with [9] and $\mathrm{eff}_{\mathrm{EUV}} = 0.5$ according to more recent studies [11]). The heating efficiencies of absorption in far UV radiation bands were calculated according to data of [11].

The cooling processes are calculated for non-LTE radiation conditions on the base of the rapid parameterization scheme (under the assumption that the emission of carbon dioxide CO_2 on the fundamental infrared band (15 m) plays the main role at these altitudes of thermosphere altitudes) [5]. The influence of the upper layers on the lower ones is neglected according to the small optical thickness of the upper thermosphere. Note that for the calculation of the concentrations of atmospheric constituents in the radiation block as well as of air density and specific heat, the diffusive separation of gas composition with altitude is considered [9, 18]. For this model version the vertical profiles of volume mixing ratios of gas species are set according to the empirical model [6].

4. REPRODUCTION OF THE THERMOSPHERIC GLOBAL STRUCTURE AND GENERAL CIRCULATION

Since the amount of observational data for the thermosphere is rather small (in contrast to the lower atmosphere), the model identification was based on comparing the results of numerical experiments on the simulated thermospheric general circulation with the results of other models (both empirical [3, 6] and numerical [17], including the first version of our model [9]) for a similar setting during equinox. Figure 1 presents the reproduction of global radiation and thermal balance for a new model of the thermosphere. The

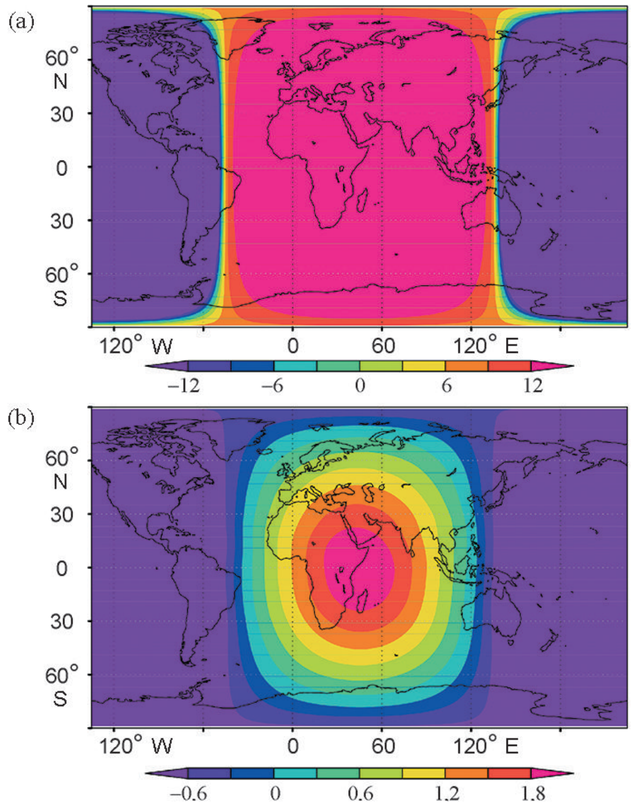

Fig. 2. Longitude-latitude distribution of calculated deviations of the heating rate (10^{-3} K/s) at the model levels of (a) p_n = = 4 10^{-6} Pa (~300 km) and (b) p_n = 2 10^{-3} Pa (~120 km) for 12:00 Moscow time (eff$_{\rm EUV}$ = 0.5, equinox).

mean vertical profile of total radiative heating of the thermosphere calculated for different values of the heating efficiency eff$_{\rm EUV}$ is shown in Fig. 1a. It is closely consistent with the empirical data and model estimates [2, 4, 16]. A decomposition analysis of different radiative forcing components for our model indicated the dominant role of absorbing EUV radiation above $p = 10^{-5}$ hPa pressure level (120 km, mean heating rate is around 100 K/day) with the maximum values of the heating rate in the upper thermosphere of about 1000 K/day (which highly depend on the parameterization settings). Heating due to the absorption of UV radiation in Schumann–Runge bands and continuum is significant for the vertical domain $10^{-3} < p < 3$ 10^{-6} hPa (from 90 to 160 km), maximum heating values being around 40 K/day. The absorption by O_2 in the Lyman-alpha line as well as by O_2, O_3 in the Herzberg continuum and Hartley bands and also the chemical heating are substantial for the narrow altitude range of 90–100 km with the heating rate values of 1–5 K/day. The calculated cooling rate due to the long-wave CO_2 emission determines the radiation balance of the lower thermosphere for the altitudes from 90 to 150 km with a maximum heat sink up to 40 K/day. These values are considerably higher than the parametrically set Newtonian cooling in the model first version (10 K/day) [9, 19]. The spatial distribution of heating rate deviations $^{-}$ for two model levels (corresponding to the altitudes of 120 km and 300 km) are presented in Fig. 2 (see Fig. 1 of [9]). In general, the main characteristics of radiation processes calculated by the new model are in good agreement with the generally accepted empirical and model estimates [9, 16, 19].

The vertical profile of the global mean temperature $\overline{T}$ calculated for different values of the key parameters of thermal balance is shown in Fig. 1b. Thus, the global state of the thermosphere is mainly determined by the ratio of radiation heating due to the absorption of EUV radiation and by heat sink due to molecular thermal conductivity (which corresponds to analytic estimates provided above (3)). Notably the closest accordance to the empirical profile has been obtained by the reduction of the conductivity coefficient by twice [3, 6]. The results of various numerical experiments indicated that the global thermal balance of lower thermosphere for this model is determined by the lower boundary conditions at the mesopause, while the values of molecular $_{\rm mol}$ and turbulent K_D heat transfer do not play a substantial role.

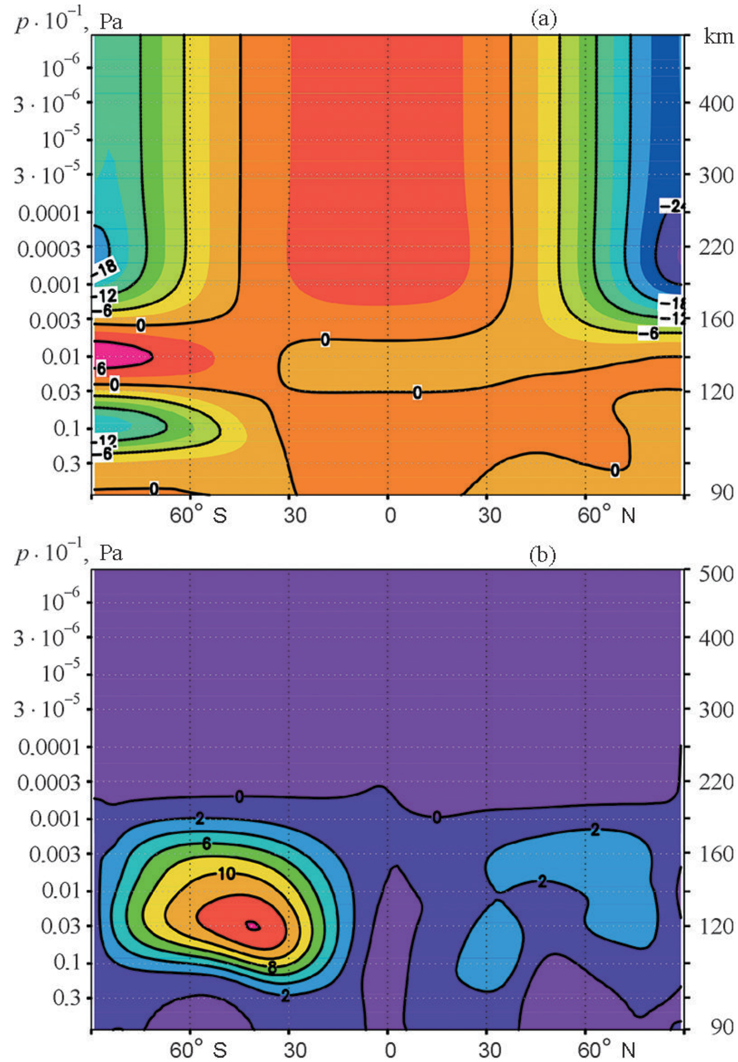

Fig. 3. (a) Zonal mean vertical profiles of temperature deviations T (K) and (b) zonal wind speed u (m/s) according to the modeling of thermospheric general circulation.

Figure 3 presents the zonal mean vertical profiles of temperature deviations from the global mean profile (Fig. 1b) and the zonal wind speed calculated with a new model of the thermosphere. Overall the established global circulation pattern is closer to the empirical estimates and model data compared to the first version of the model (see Fig. 2 of [9] and Fig. 2 of [16]). There is no strong polar overcooling in the lower layers, and the meridional temperature gradient is in good agreement with the empirical data [3, 6], thereby the zonal transport in the lower thermosphere is reproduced more accurately. Figure 4 shows the horizontal spatial distribution of temperature deviations for 120 km and 300 km that demonstrate the reproduction of thermospheric tides (see Fig. 3 of [9] and Fig. 4 of [16]). The amplitudes of the diurnal tide (around 100 K at the equator) and its structure in the upper atmosphere correspond well to empirical data for considered conditions [3, 6] indicating a good reproduction of the balance of radiative and dynamical processes. The tidal amplitudes of the lower thermosphere are significantly underestimated in comparison with the results of the first version [9] and other data [16] (the maximum values are up to 10 K compared with 25–30 K), while the spatial structure of diurnal and semidiurnal tides is reproduced fairly accurately. The main errors in the reproduction of the lower thermospheric circulation (lack of non-migrating tides, etc.) are associated primarily with the inaccurate description of heat sink due to turbulent diffusion and the neglect of wave disturbances propagating from the mesosphere. In addition, the general shortcomings of the reproduction of the global thermospheric circulation structure are caused by the lack of account of the diurnal variation of

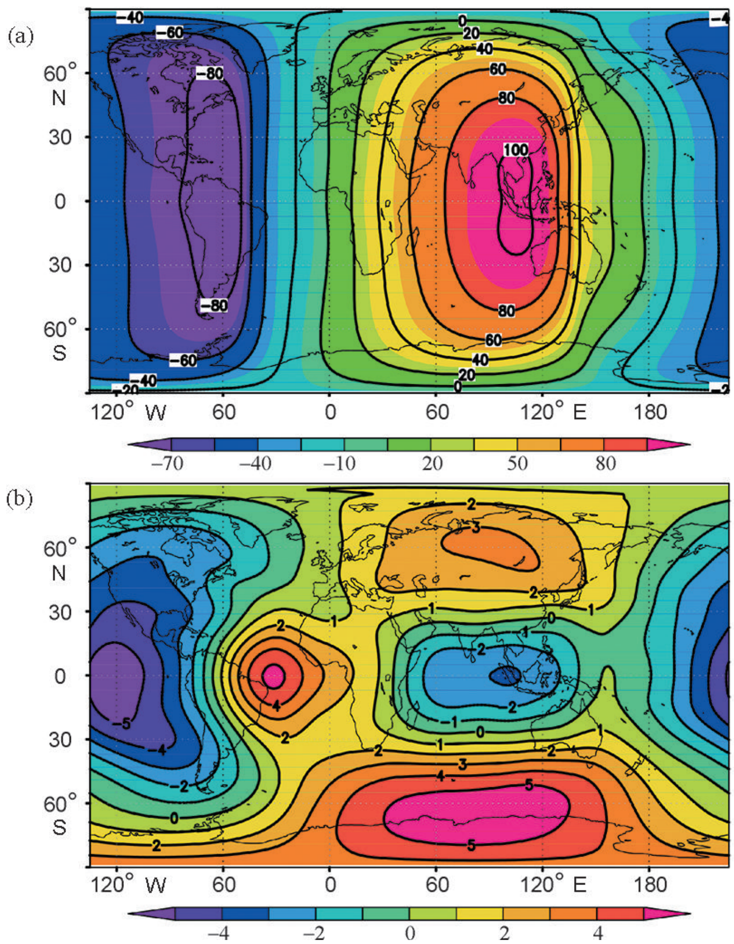

Fig. 4. The same as in Fig. 2 for temperature deviations T (K).

ionospheric parameters and the precipitation of energetic particles in the polar regions as well as by the lack of consistent description of photochemical transformations [3, 16, 17].

The further development of the model will focus on the constructing of the coupled model of the thermosphere and lower atmosphere in order to eliminate significant inaccuracies in the reproduction of the thermospheric circulation at the altitudes close to the mesosphere. It should be noted that these inaccuracies arise because the present version of the model neglects interaction with the mesosphere.

ACKNOWLEDGMENTS

This work was performed at INM RAS and was supported by the Russian Science Foundation (grant 14-27-00126).

REFERENCES

1. G. I. Marchuk, V. P. Dymnikov, and V. B. Zalesny, *Mathematical Modeling of the General Circulation of the Atmosphere and Ocean* (Gidrometeoizdat, Leningrad, 1984) [in Russian].
2. S. Chandra and A. K. Sinha, "The Role of Eddy Turbulence in the Development of Self-consistent Models of the Lower and Upper Thermospheres," J. Geophys. Res., No. 3, **79** (1973).
3. M. V. Codrescu, T. J. Fuller-Rowell, et al., "Validation of the Coupled Thermosphere Ionosphere Plasmasphere Electrodynamics Model: CTIPE-Mass Spectrometer Incoherent Scatter Temperature Comparison," Space Weather, No. 9, **6** (2008).
4. R. E. Dickinson, E. C. Ridley, and R. G. Roble, "A Three-dimensional General Circulation Model of the Thermosphere," J. Geophys. Res., **86** (1981).

5. V. I. Fomichev, A. A. Kutepov, R. A. Akmaev, and G. M. Shved, “Parameterization of the 15 m CO_2 Band Cooling in the Middle Atmosphere,” J. Atmos. and Solar-Terr. Phys., **55** (1993).
6. A. E. Hedin, “Extension of the MSIS Thermosphere Model into the Middle and Lower Atmosphere,” J. Geophys. Res., No. A2, **96** (1991).
7. C. O. Hines, “Doppler Spread Parameterization of Gravity Wave Momentum Deposition in the Middle Atmosphere. Part 1, Basic Formulation,” J. Atmos. Terr. Phys., No. 4, **59** (1997).
8. T. L. Killeen, “Energetics and Dynamics of the Earth’s Thermosphere,” Rev. Geophys., No. 3, **25** (1987).
9. D. V. Kulyamin and V. P. Dymnikov, “A Three-dimensional Model of General Thermospheric Circulation,” Russ. J. Numer. Anal. and Math. Modelling, No. 4, **28** (2013).
10. D. V. Kulyamin and V. P. Dymnikov, “The Atmospheric General Circulation Model with a Hybrid Vertical Coordinate,” Russ. J. Numer. Anal. and Math. Modelling, No. 6, **29** (2014).
11. M. G. Mlynczak and S. Solomon, “A Detailed Evaluation of the Heating Efficiency in the Middle Atmosphere,” J. Geophys. Res., No. D6, **98** (1993).
12. A. I. Pogoreltsev, A. A. Vlasov, K. Frohlich K., and Ch. Jacobi, “Planetary Waves in Coupling the Lower and Upper Atmosphere,” J. Atmos. Solar-Terr. Phys., **69** (2007).
13. M. Reise, D. Offermann, and G. Brasseur, “Energy Released by Recombination of Atomic Oxygen and Related Species at Mesopause Heights,” J. Geophys. Res., No. D7, **99** (1994).
14. P. G. Richards, J. A. Fennelly, and D. G. Torr, “EUVAC: A Solar EUV Flux Model for Aeronomic Calculations,” J. Geophys. Res., No. A5, **99** (1994).
15. P. G. Richards, M. R. Torr, and D. G. Torr, “Solar EUV Energy Budget of the Thermosphere,” Adv. Space Res., No. 12, **1** (1981).
16. R. G. Roble, “The Calculated and Observed Diurnal Variation of the Ionosphere over Millstone Hill on March 23–24, 1970,” Planet Space Sci., No. 7, **23** (1975).
17. R. G. Roble, E. C. Ridley, and R. E. Dickinson, “On the Global Mean Structure of the Thermosphere,” J. Geophys. Res., **92** (1987).
18. R. W. Schunk and A. Nagy, *Ionospheres: Physics, Plasma Physics, and Chemistry* (Cambridge University Press, 2009).
19. K. P. Shine, J. A. Ricaby, *Solar Radiative Heating due to Absorption by Ozone* (Department of Atmospheric, Oceanic and Planetary Physics, University of Oxford, Oxford, UK, 1989).
20. R. S. Stolarski, P. B. Hays, and R. G. Roble, “Atmospheric Heating by Solar EUV Radiation,” J. Geophys. Res., No. 16, **80** (1975).
21. D. F. Strobel, “Parameterization of the Atmospheric Heating Rate from 15 to 120 km due to O_2 and O_3 Absorption of Solar Radiation,” J. Geophys. Res., No. 12, **83** (1978).